ELSEVIER

Earth and Planetary Science Letters 194 (2002) 359–368

EPSL

www.elsevier.com/locate/epsl

Magnetic field control of the low-temperature magnetic properties of stoichiometric and cation-deficient magnetite

Alexei V. Smirnov, John A. Tarduno *

Department of Earth and Environmental Sciences, University of Rochester, Rochester, NY, USA

Received 21 September 2001; received in revised form 2 November 2001; accepted 2 November 2001

Abstract

We report three new types of low-temperature (<120 K) magnetic behavior from oxidized and stoichiometric pseudo-single domain magnetite: (1) a non-monotonic dependence of the saturation remanence to saturation magnetization ratio on the magnetic field (0–1.7 T) applied during cooling, (2) an induced magnetic anisotropy at temperatures below the transition from cubic to monoclinic crystalline symmetry at $\sim$120 K (the Verwey transition) after cooling in magnetic fields between 0.01 and 0.09 T, and (3) a non-monotonic dependence of a low-temperature (10 K) remanent magnetization on the magnetic field (0.01–2.5 T range) applied during cooling through the Verwey transition. We interpret these phenomena in terms of relationships between crystal twins, that can form in monoclinic magnetite, and the reorganization of magnetic domains. Our results are important for interpretations of low-temperature magnetic measurements and provide new insight into the fundamental magnetic properties of magnetite at low temperatures. © 2002 Published by Elsevier Science B.V.

Keywords: magnetite; crystal systems; magnetic hysteresis; twinning

1. Introduction

Low-temperature magnetic measurements have been increasingly utilized in rock- and paleomagnetism for magnetic mineral diagnostics and granulometry [1–5]. Interpretations of these data, however, are ultimately based on our understanding of the basic magnetic properties of minerals at cryogenic temperatures. Of special interest is magnetite (Fe_3O_4) which, by virtue of its isotropic point at $\sim$130 K [6] and its transition from cubic to monoclinic crystalline symmetry at $\sim$120 K (T_V, the Verwey transition) [7], is easily recognizable in low-temperature magnetic data [8].

It has long been known that the application of a strong magnetic field during cooling through the Verwey transition affects magnetic properties of the monoclinic phase of magnetite [9]. A few studies have further investigated the effect of the magnetic field on magnetic hysteresis at low temperatures [10,11]. In these studies, cooling in a zero field was compared to cooling in a very strong field (>1.5 T). Overall, the experimental database on magnetic hysteresis properties at low temperatures is small (e.g. [12–15]). Another important factor is the effect of oxidation, which results in cation-deficient magnetite ($Fe^{3+}_{2+2z/3}Fe^{2+}_{1-z}\square_{z/3}O^{2-}_4$)

* Corresponding author. Tel.: +1-585-275-8810; Fax: +1-585-244-5689.
E-mail address: alexei@earth.rochester.edu (J.A. Tarduno).

0012-821X/02/$ – see front matter © 2002 Published by Elsevier Science B.V.
PII: S0012-821X(01)00575-1

common in natural samples. Unfortunately, the low-temperature database for cation-deficient magnetite is even smaller than that for stoichiometric magnetite [16,17].

To contribute to these databases, we report experimental results on low-temperature magnetic hysteresis properties of magnetite as a function of the magnetic field applied during cooling. We have studied samples of oxidized and stoichiometric pseudo-single domain (PSD) magnetite. Low-temperature magnetic measurements were performed at the Institute of Rock Magnetism (University of Minnesota). Through these studies we have discovered several new types of low-temperature magnetic behavior. Below we describe these magnetic properties and offer some interpretations in terms of processes occurring at and below the Verwey transition.

2. Sample preparation and oxidation state

The first sample studied was a synthetic magnetite powder W3006 produced by Wright Industries, Inc. The grain size reported for this powder is 2–3 μm. We examined the powder with a low-voltage high-resolution LEO 982 scanning electron microscope (SEM) at the University of Rochester. We found the grain sizes ranged from 0.5 to 6.5 μm, approximating a log-normal distribution with an apparent mean grain size of $\sim$1.5 μm. A second sample was prepared by reducing magnetite W3006 in a CO/CO_2 (1:10) atmosphere at 400°C for 4 h. High-resolution SEM analyses indicate no significant change in grain size after reduction. Magnetic hysteresis properties (saturation magnetization, M_s; saturation remanence, M_{rs}; coercivity, H_c; coercivity of remanence, H_{cr}) were measured at room temperature. Both non-reduced ($H_c = 23.3$ mT, $H_{cr} = 39.0$ mT, $H_{cr}/H_c = 1.67$, $M_{rs}/M_s = 0.263$) and reduced ($H_c = 12.7$ mT, $H_{cr} = 24.6$ mT, $H_{cr}/H_c = 1.94$, $M_{rs}/M_s = 0.169$) samples show PSD behavior [18].

To characterize the oxidation state of the samples, Mössbauer spectra were measured in a zero magnetic field environment using a Ranger Scientific Mössbauer Spectrometer with a ^{57}Co source. The zero field room temperature Mössbauer spectrum for magnetite consists of two sextets, related to Fe-cations in tetrahedrally coordinated (A) and octahedrally coordinated (B) sites of the inverse spinel lattice (e.g. [19]). For stoichiometric magnetite, the relative ratio (A/B) of the two spectral components should be close to 1:1.88 [20,21]. For cation-deficient magnetite the ratio increases with oxidation parameter z [20]. For our non-reduced and reduced samples the A/B ratios were 0.494/0.518 (1:1.05) and 0.327/0.621 (1:1.90), respectively. These data indicate that magnetite W3006 is oxidized, and was reduced to stoichiometric magnetite by the controlled-atmosphere heating described above.

Oxidation parameters were determined through X-ray diffraction measurements using a Scintag X-ray diffractometer XDS-2000 at the University of Rochester. The lattice parameter a was calculated using eight peaks corresponding to diffractions by planes (220) to (533). A half-angle between the diffracted beam and the incident X-ray beam was changed from 29° to 44°. The parameter a for the reduced magnetite is 8.396 ± 0.001, indistinguishable from that of stoichiometric magnetite ($z = 0$) [22]. For the non-reduced magnetite $a = 8.390 \pm 0.001$, corresponding to an oxidation parameter $z = 0.24$ [23]. Mass-normalized saturation magnetizations measured from the reduced and non-reduced magnetite at room temperature were 91.3 and 87.2 Am^2/kg, respectively, supporting the results of Mössbauer and X-ray diffraction analyses.

3. Experimental results

3.1. Thermal demagnetization of low-temperature saturation remanence

Thermal demagnetization of low-temperature saturating isothermal remanent magnetization (LT SIRM) was measured using a Quantum Design Magnetic Property Measurement System (MPMS-XL). First, samples were demagnetized in an alternating magnetic field (AF) of 0.2 T and cooled from 300 to 10 K either in a zero magnetic field or in a magnetic field between 0.05 and 2.5 T. At 10 K, a 2.5 T direct magnetic

field was applied for 60 s to impart a LT SIRM. Thermal demagnetization of the LT SIRM was measured at 5 K intervals during zero field warming to room temperature (Fig. 1). The Verwey transition for the non-reduced magnetite is blurred and shifted to lower temperatures, typical of oxidized magnetite with $z < 0.3$ [16]. The sharp transition observed at $\sim$120 K from the reduced magnetite further indicates its high stoichiometry.

Interestingly, the strength of the LT SIRM depends on the magnetic field applied during cooling (H_V) in a non-monotonic fashion: the LT SIRM imparted after field cooling (FC) in 0.05 and 0.2 T is considerably higher than that imparted after FC in 2.5 T. The latter value is nearly equal to the LT SIRM imparted after zero field cooling (ZFC) for the stoichiometric magnetite (Fig. 1b). For the cation-deficient magnetite, the LT SIRM imparted after FC in 2.5 T is lower than that imparted after ZFC (Fig. 1a). These results suggest a complex field-dependence of M_{rs}/M_s for the monoclinic magnetite phase. To further explore this, we measured magnetic hysteresis properties as a function of H_V.

3.2. Magnetic field-dependence of magnetic hysteresis parameters

Cation-deficient and stoichiometric magnetites were AF-demagnetized at 300 K and cooled to 10 K in a zero field and in the presence of 0.2 T and 1.7 T magnetic fields. At 10 K, magnetic hysteresis loops were measured (maximum applied field $H_{max} = 1.7$ T) using a Princeton measurements variable-temperature vibrating sample magnetometer. Although some studies suggest that magnetite may not be fully saturated in a 1.7 T field at very low temperature (e.g. [8]), the difference between measured and true M_s values has been shown to be only a few percent [11]. To determine H_{cr}, DC demagnetization curves were measured. An unusual non-monotonic dependence of the M_{rs}/M_s ratio on the field H_V was observed for both samples (Table 1). Cooling of the cation-deficient magnetite in an intermediate 0.2 T magnetic field results in a $M_{rs}/M_s \sim 14\%$

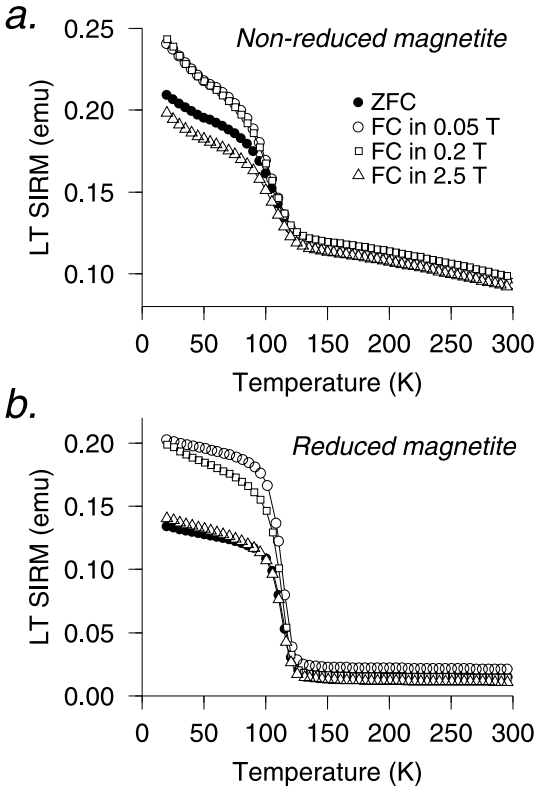

Fig. 1. Thermal demagnetization of saturation isothermal remanent magnetization imparted at 10 K after ZFC (solid circles) and FC (open symbols). (a) Cation-deficient magnetite. (b) Stoichiometric magnetite.

Table 1
Magnetic hysteresis parameters at 10 K after zero field cooling and field cooling

	Cation-deficient magnetite			Stoichiometric magnetite		
	ZFC	FC 0.2 T	FC 1.7 T	ZFC	FC 0.2 T	FC 1.7 T
M_{rs}/M_s	0.333	0.409	0.358	0.275	0.405	0.307
H_c (mT)	42.2	31.7	28.3	31.2	23.0	19.5
H_{cr} (mT)	66.0	44.0	42.4	52.2	27.6	23.3
H_{cr}/H_c	1.56	1.39	1.50	1.67	1.20	1.19

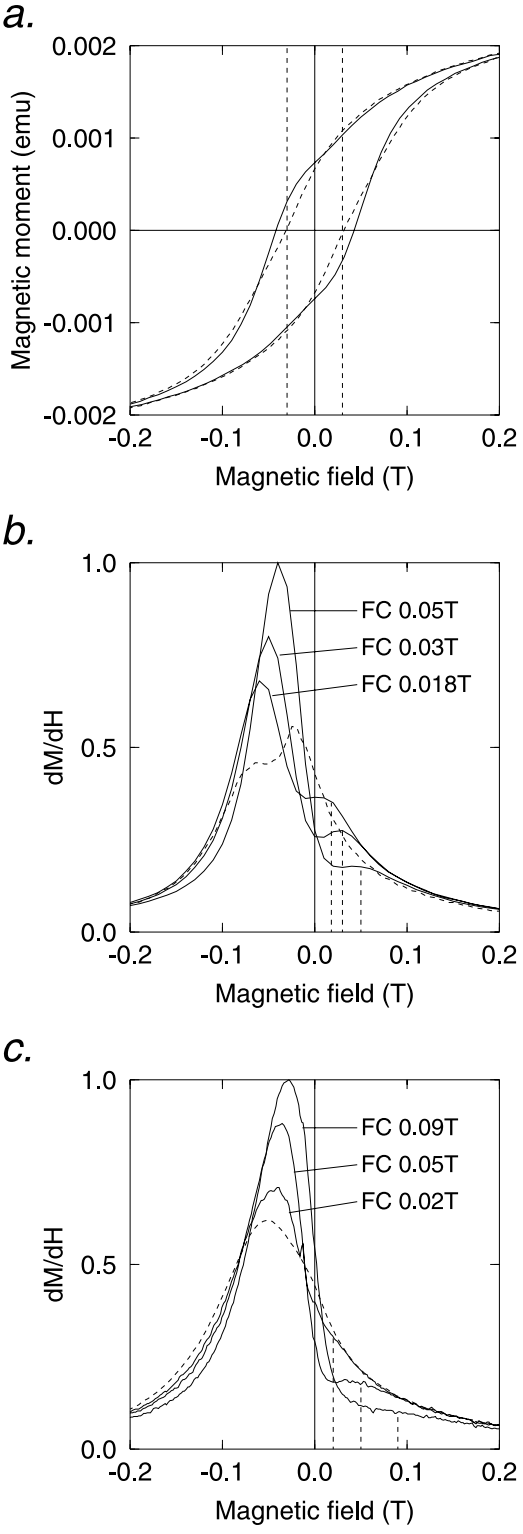

greater than that measured after cooling in a stronger 1.7 T field, and ~23% greater than that measured after zero field cooling (ZFC). This effect is more pronounced for stoichiometric magnetite (the respective values are ~32% and ~47%). For both samples, H_c and H_{cr} are greatest after ZFC and decrease as the field H_V increases (Table 1).

3.3. Magnetic field-memory effect

Another unexpected result of the magnetic hysteresis measurements was the observation that both minor ($H_{max} = 0.2$ T) and saturated ($H_{max} = 1.7$ T) loops measured at 10 K have an inflection point located at the field H_V (Fig. 2a). Because the field H_V can be determined by measuring a low-temperature hysteresis loop, we call this phenomena a field-memory effect. This effect is distinct from the low-temperature memory when part of a remanence survives low-temperature demagnetization by cycling through the Verwey transition [22]. The inflection point is better seen on the first derivative (dM/dH) of a hysteresis loop as a local maximum located at the field H_V (Fig. 2b). To check the reproducibility of the effect, hysteresis loops were measured after subsequent coolings in a magnetic field of different magnitudes (0.01–0.09 T) applied in random order. A perfect correlation between H_V and the location of the inflection point was observed (Fig. 2). For fields $H_V > 0.1$ T the field-memory

←

Fig. 2. Effect of memory of a magnetic field applied during cooling through the Verwey transition. (a) Magnetic hysteresis loops (central parts are shown only) measured at 10 K from stoichiometric magnetite after ZFC (dashed curve) and cooling in 0.03 T magnetic field (FC, solid curve). Vertical dashed lines show a 0.03 T field where an inflection point is observed both on descending and ascending branches of the field cooled loop. (b) First derivatives of hysteresis loops (descending branches only) measured at 10 K from stoichiometric magnetite after ZFC (dashed curve), and after FC (solid curves). The location of the inflection points (a local maximum on a dM/dH curve) correlate with the magnetic field of cooling (vertical dashed lines). (c) First derivatives of hysteresis loops (descending branches only) measured at 10 K on cation-deficient magnetite after ZFC (dashed curve) and after FC (solid curves).

effect was not observed. Interestingly, for the stoichiometric magnetite, hysteresis loops measured after ZFC also manifest some distortion (Fig. 2b), having two maxima on a dM/dH curve. However, in contrast to a field cooling (FC), both maxima are located on one side of the H-axis. For the cation-deficient magnetite the field-memory effect is observed within a narrower range of H_V (0.02–0.09 T) (Fig. 2c) and a loop measured after ZFC shows no distortion (Fig. 2c).

To constrain the temperature interval where processes responsible for the field-memory effect occur we used a partial field cooling technique [4]. The field-memory effect was observed only if the magnetic field H_V was applied during cooling through the Verwey transition. We also studied the temperature dependence of the field-memory effect by measuring hysteresis loops at 5 K steps with increasing temperature from 10 to 150 K. The field-memory effect survives heating up to $\sim$110 K, but completely disappears after $\sim$125 K. These experiments suggest that the presence of the Verwey transition is a necessary factor for the field-memory effect. This is further supported by the fact that we observed no field-memory effect for a sample of PSD maghemite, which also showed no low-temperature transition.

To investigate directional anisotropy of the field-memory effect, magnetic hysteresis loops (at 10 K) were measured at different angles (15° increment) with respect to the direction of H_V (0.03 T). An uniaxial anisotropy of the field-memory effect was observed: an inflection point at H_V is best seen at 0° and 180° and is not observable at 90° and 270° (Fig. 3). Interestingly, the inflection point at H_V is blurred at 360° suggesting that multiple applications of strong magnetic fields in opposed directions affects the features responsible for the field-memory effect.

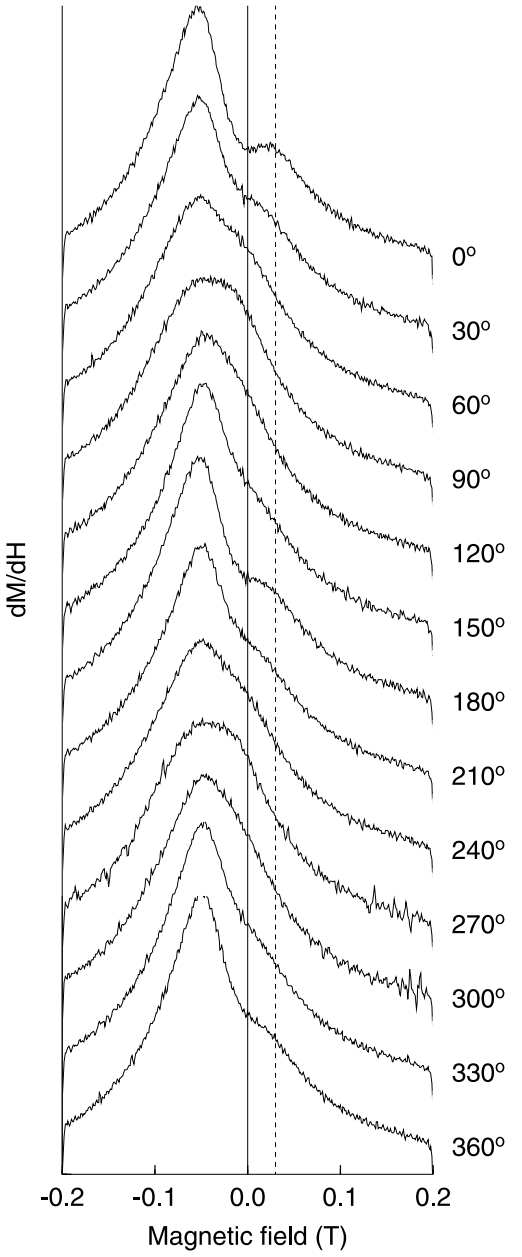

Fig. 3. Angular dependence of the field-memory effect induced in 0.03 T (vertical dashed line). First derivatives of hysteresis loops (descending branches only) measured at 10 K from stoichiometric magnetite are shown.

3.4. Low-temperature transitional remanent magnetization (LT TrRM)

Motivated by our LT SIRM and magnetic hysteresis results, we studied some additional characteristics of the remanent magnetization acquired when a magnetite sample is cooled through the Verwey transition in the presence of a magnetic field. We call this magnetization a low-temperature transitional remanent magnetization (LT TrRM). Again, samples were AF-demagnetized at 300 K and cooled to 10 K in the presence of

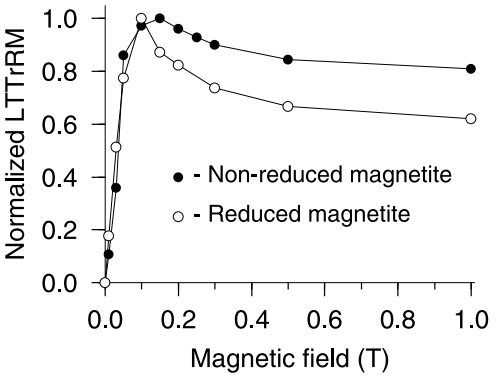

Fig. 4. Dependence of LT TrRM on magnetic field for cation-deficient (solid circles) and stoichiometric (open circles) magnetite.

a magnetic field H_V. During cooling, an induced magnetization was measured using the MPMS-XL. At 10 K, the magnetic field was turned off and the remanent magnetization (LT TrRM) measured. Next, thermal demagnetization of the LT TrRM was measured at 5 K intervals to 300 K in a zero field. These measurements were done for several magnetic fields H_V (0.01–2.5 T). In contrast to other magnetizations, which show a monotonic increase with a magnetic field to a saturation level, the LT TrRM manifests an unusual non-monotonic dependence on H_V. For stoichiometric magnetite, LT TrRM has a maximum at $\sim$0.10 T and decreases by $\sim$38% to a stable level at $\sim$1 T. For cation-deficient magnetite the maximum is shifted to a slightly higher field ($\sim$0.15 T) and the subsequent decrease of LT TrRM to a stable level at $\sim$1 T is $\sim$20% (Fig. 4).

4. Discussion

In our study special care was taken to control the magnetic mineralogy and oxidation state of studied samples. No secondary magnetic phases were found using Mössbauer and X-ray diffraction analyses. A bimodal grain size distribution which could cause a distortion of hysteresis loops was not observed in our SEM analyses and is not supported by magnetic hysteresis data at room temperature: for both cation-deficient and stoichiometric magnetite hysteresis loops are not distorted. The blocking of superparamagnetic (SP) grains is unlikely to be responsible for the phenomena observed because (i) the shape of the distorted loops does not change on warming from 10 K to 110 K and (ii) the field-memory effect would be better pronounced for oxidized magnetite with cracked maghemite coatings behaving as SP particles [16]. A physical rotation of magnetic grains in a strong magnetic field as a possible cause of the observed effects was excluded by control experiments on magnetite powders fixed in epoxy.

The phenomena observed are more pronounced for our stoichiometric magnetite sample, indicating that processes related to low-temperature transitions must play a causal role. The domain structure of magnetite is reorganized when cooled below its isotropic point where the magnetocrystalline anisotropy constant K_1 changes sign (e.g. [24]). Monoclinic crystal twins can form when magnetite cools through the Verwey transition [25]. Twinning has been observed in a wide range of magnetite sizes including very large synthetic plates (0.18 mm$\times$5 mm$\times$7 mm) (e.g. [26,27]) and very small (50–100 nm) natural grains (e.g. [28]). Domain wall reorganization and monoclinic crystal twin formation may be interrelated in a way that gives rise to the low-temperature phenomena we have observed.

Strain related to magnetostriction is high near magnetic domain walls favoring the nucleation of twin boundaries [25,29,30]. Therefore, the distribution of twin boundaries may be controlled by the magnetic domain configuration formed upon passing T_V in an applied field (H_V). On the other hand, zones of maximum strain and dislocations associated with twin boundaries [25] may create potential energy barriers which hinder the motion of the magnetic domain walls during the field cycling used in magnetic hysteresis measurements (e.g. [31]). After a magnetic domain wall is moved by remagnetization from its position previously determined on cooling in the field H_V, this location is 'remembered' by the overall configuration of twin boundary defects. The field-memory effect (Fig. 2), therefore, is a result of a slower, or inhibited, remagnetization near the initial applied field value (H_V) which is manifested as a distortion in magnetic hysteresis curves.

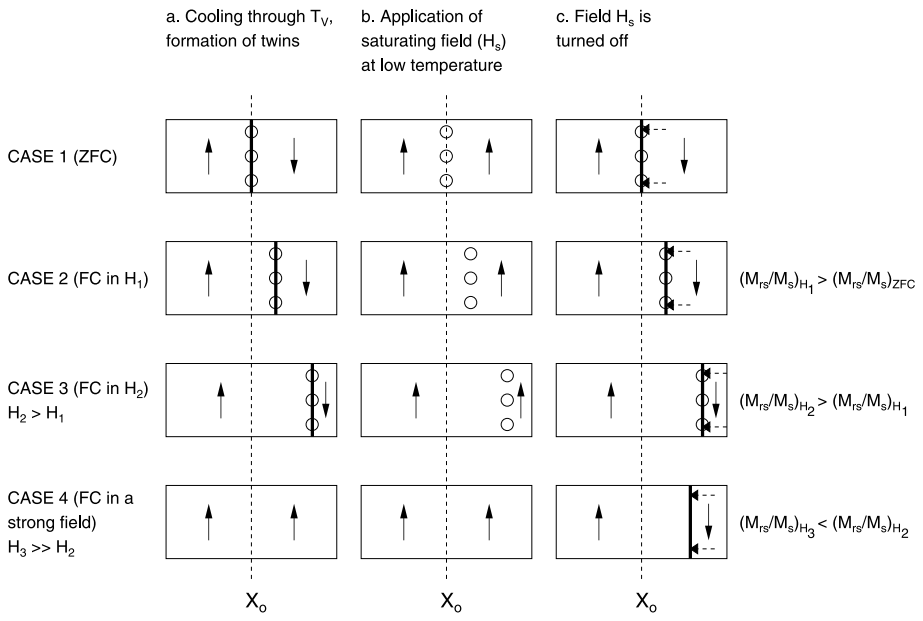

Fig. 5. Schematic representation of remagnetization in a simplified two-domain system (domain magnetization direction is shown by thin arrows). X_0 shows the location of a domain wall corresponding to the demagnetized state. (a) Twin boundaries defects (circles) form at or near the position of a domain wall as magnetite is cooled through the Verwey transition (T_V). (b) A strong magnetic field (H_s) is applied at a low temperature ($T < T_V$) so that the system is completely remagnetized. (c) The field H_s is turned off. Short arrows indicate sense of domain wall motion. Relative values of the ratio of saturation remanence to saturation magnetization (M_{rs}/M_s) are also shown. The twin boundary defects (cases 1–3) pin domain walls. Case 1: ZFC. Twin boundaries defects concentrate around X_0. Case 2: FC in an intermediate magnetic field H_1. The magnetic domain wall and twin boundary defects are shifted from X_0. Case 3: FC in a magnetic field $H_2 > H_1$. The magnetic domain wall and twin boundary defects are located further from X_0 than in case 2. Case 4: FC in a strong magnetic field $H_3 \gg H_2$ where a magnetic domain wall does not nucleate. Twin boundary defects also do not form.

We also suggest that the interaction between the magnetic domain structure and twin formation is an important factor determining the non-monotonic behavior of the M_{rs}/M_s ratio (Table 1). When H_V is zero or relatively small (so that magnetic domain walls are present), the M_{rs}/M_s ratio at temperature below T_V is predominantly controlled by twin boundary defects. After ZFC, a magnetic domain wall forms at the demagnetized position (X_0) and, hence, twin boundary defects concentrate around X_0 (e.g. case 1, Fig. 5). If we consider cooling in higher fields, magnetic domain walls and twin boundary defects will be located further from X_0 (cases 2 and 3, Fig. 5). Therefore, after a saturating field H_s (applied to measure M_{rs}) is turned off, a domain wall will be pinned in the position corresponding to a higher M_{rs}, resulting in a higher M_{rs}/M_s ratio.

Next we consider the situation when the field applied during cooling (H_V) is high enough to saturate the samples of interest (case 4, Fig. 5). In this case, no domain walls form so that even if twinning occurs, the location of twin boundaries is not determined by the domain structure. Therefore, after H_s is turned off, domain walls are not pinned by twin boundary defects and the value of M_{rs} may be lower than that measured after cooling in smaller applied fields (Fig. 5, cases 3 and 4). However, the M_{rs}/M_s ratio is still higher than that measured after ZFC (Table 1). This observation is consistent with results reported elsewhere [10,11] and may be explained by an alignment of the monoclinic easy magnetization axes (*c*-axes). When cooled in the presence of a strong magnetic field the monoclinic *c*-axes are thought to form along the [001] direction of the cubic plane closest to the applied field direction so that they are uniformly distributed within a cone around the field

direction applied during cooling [32,33]. We suggest that the alignment of *c*-axes becomes a dominate factor controlling the M_{rs}/M_s ratio if the field applied during cooling (H_V) is strong enough to nearly saturate monoclinic magnetite.

Interestingly, a monotonic decrease of H_{cr} with the magnetic field applied during cooling (H_V) is observed both for stoichiometric and non-stoichiometric magnetites. The values of H_{cr} after cooling in applied fields of 0.2 and 1.7 T do not differ greatly (Table 1). As a first approximation, the coercivity of remanence is directly proportional to the amount of defects in a magnetic crystalline lattice. Therefore, the decrease of H_{cr} may be due to a smaller number of twin boundaries forming in a crystal because of the alignment of *c*-axes with progressively higher applied fields H_V. The decreased number of twin boundary defects may account for the less pronounced field-memory effect observed for higher H_V (Fig. 2).

The interrelationship between monoclinic twin boundaries in magnetite and domain walls may also explain the non-monotonic behavior of LT TrRM. For an intermediate applied field (H_V), formation of defects due to monoclinic twinning promotes a stronger pinning of magnetic domain walls resulting in a higher LT TrRM. For stronger H_V, when the amount of defects decreases (because twinning decreases), pinning becomes weaker. The remanence drops to lower values after the field H_V is turned off.

Our interpretation based on the presence of monoclinic twin boundary defects in magnetite may also explain other experimental observations. The uniaxial anisotropy of the field-memory effect results from the dominance of 180° magnetic domain neighborhoods in monoclinic magnetite (e.g. [34]). Blurring of the field-memory effect observed after multiple application of a magnetic field (Fig. 3) may be explained by the fact that the twin boundaries themselves can be moved by a magnetic field, although at a much slower rate than magnetic domain walls [30]. On a final note it is interesting to mention that the non-monotonic behavior of field-dependence of LT TrRM resembles the field-dependence of TRM for some types of spin glasses (e.g. [35,36]).

5. Conclusion

Our experimental results show that the magnetic properties of magnetite at low temperatures depend on the magnetic field applied during cooling. The following phenomena were observed:

1. A non-monotonic dependence of M_{rs}/M_s on a magnetic field (0–1.7 T) applied during cooling.
2. An induced uniaxial anisotropy (field-memory effect) after cooling through the Verwey transition in magnetic fields between 0.01 and 0.09 T.
3. A non-monotonic field-dependence of low-temperature transitional remanent magnetization within the field interval 0.01 to 2.5 T.

The observed phenomena appear to have their origin in complex interrelationships between the formation of crystal twins in monoclinic magnetite and domain wall movements. While more experimental and theoretical studies are needed, the observations described should be considered when interpreting low-temperature magnetic data commonly used in rock- and paleomagnetic applications. Furthermore, these new results may be useful in studying planets and their satellites where magnetite subjected to very low temperatures and relatively strong magnetic fields may be present.

Acknowledgements

We thank Brian Carter-Stiglitz for help with reduction experiments, Peter Solheid for conducting Mössbauer experiments, Pavel Doubrovine for measuring X-ray diffraction spectra, and Andrei Kosterov for review of the manuscript. A.S. thanks the Institute of Rock Magnetism (IRM, University of Minnesota) for a Visiting Fellowship. Funds for the IRM were provided by the Keck Foundation and the University of Minnesota. Overall support for this research at the University of Rochester was provided by the National Science Foundation. *[RV]*

References

[1] I. Snowball, M. Torii, Incidence and significance of magnetic iron sulfides in Quaternary sediments and soils, in: B.A. Maher, R. Thompson (Eds.), Quaternary climates, environments and magnetism, Cambridge University Press, Cambridge, 1999, pp. 199–230.

[2] S.K. Banerjee, C.P. Hunt, X.-M. Liu, Separation of local signals from the regional paleomonsoon record of the loess plateau: A rock-magnetic approach, Geophys. Res. Lett. 20 (1993) 843–846.

[3] J.A. Tarduno, Superparamagnetism and reduction diagenesis in pelagic sediments: enhancement or depletion?, Geophys. Res. Lett. 22 (1995) 1337–1340.

[4] A.V. Smirnov, J.A. Tarduno, Low-temperature magnetic properties of pelagic sediments (Ocean Drilling Program Site 805C): Tracers of maghemitization and magnetic mineral reduction, J. Geophys. Res. 105 (2000) 16457–16471.

[5] B.M. Moskowitz, R.B. Frankel, D.A. Bazylinski, Rock magnetic criteria for the detection of biogenic magnetite, Earth Planet. Sci. Lett. 120 (1993) 283–300.

[6] Y. Syono, Magnetocrystalline anisotropy and magnetostriction of Fe_3O_4-Fe_2TiO_4 series – with special application to rock magnetism, Jpn. J. Geophys. 4 (1965) 71–143.

[7] E.J.W. Verwey, Electron conduction of magnetite (Fe_3O_4) and its transition point at low temperatures, Nature 144 (1939) 327–328.

[8] A.R. Muxworthy, E. McClelland, Review of the low-temperature magnetic properties of magnetite from a rock magnetic perspective, Geophys. J. Int. 140 (2000) 101–114.

[9] C.H. Li, Magnetic properties of magnetite crystals at low temperature, Phys. Rev. 40 (1932) 1002–1012.

[10] E. Schmidbauer, R. Keller, Magnetic properties and rotational hysteresis of Fe_3O_4 and g-Fe_2O_3 particles $\sim$250 nm in diameter, J. Magn. Magn. Mater. 152 (1996) 99–108.

[11] A.A. Kosterov, Magnetic hysteresis of pseudo-single-domain and multidomain magnetite below the Verwey transition, Earth Planet. Sci. Lett. 186 (2001) 245–253.

[12] A.H. Morish, L.A.K. Watt, Coercive force of iron oxide micropowders at low temperatures, J. Appl. Phys. 29 (1958) 1029–1033.

[13] E. Schmidbauer, N. Schembera, Magnetic hysteresis properties and anhysteretic remanent magnetization of spherical Fe_3O_4 particles in the grain size range 60–160 nm, Phys. Earth Planet. Inter. 46 (1987) 77–83.

[14] Ö. Özdemir, D.J. Dunlop, Low-temperature properties of a single crystal of magnetite oriented along principal magnetic axes, Earth Planet. Sci. Lett. 165 (1999) 229–239.

[15] A.R. Muxworthy, Low-temperature susceptibility and hysteresis of magnetite, Earth Planet. Sci. Lett. 169 (1999) 51–58.

[16] Ö. Özdemir, D.J. Dunlop, B.M. Moskowitz, The effect of oxidation on the Verwey transition in magnetite, Geophys. Res. Lett. 20 (1993) 1671–1674.

[17] Y. Cui, K.L. Verosub, A.P. Roberts, The effect of low-temperature oxidation on large multi-domain magnetite, Geophys. Res. Lett. 21 (1994) 757–760.

[18] R. Day, M. Fuller, V.A. Schmidt, Magnetic hysteresis properties of synthetic titanomagnetites, J. Geophys. Res. 81 (1976) 873–880.

[19] L. Häggström, H. Annersten, T. Ericsson, R. Wäppling, W. Karner, S. Bjarman, Magnetic dipolar and electric quadrupolar effects on the Mössbauer spectra of magnetite above the Verwey transition, Hyp. Inter. 5 (1978) 201–214.

[20] G.M. Da Costa, E. De Grave, P.M.A. De Bakker, R.E. Vandenberghe, Influence of nonstoichiometry and the presence of maghemite on the Mössbauer spectrum of magnetite, Clays Clay Miner. 45 (1995) 656–668.

[21] G.A. Sawatzky, F. van der Woude, A.H. Morrish, Recoilless-fraction ratios for Fe^{57} in octahedral and tetrahedral sites of a spinel and a garnet, Phys. Rev. 183 (1969) 383–386.

[22] D.J. Dunlop, Ö. Özdemir, Rock Magnetism: Fundamentals and frontiers, Cambridge University Press, Cambridge, 1997, 573 pp.

[23] P.W. Readman, W. O'Reilly, Magnetic properties of oxidized (cation-deficient) titanomagnetites (Fe,Ti,□)O_4, J. Geomagn. Geoelectr. 24 (1972) 69–90.

[24] S.L. Halgedahl, R.D. Jarrard, Low-temperature behavior of single-domain through multidomain magnetite, Earth Planet. Sci. Lett. 130 (1995) 127–139.

[25] A. Putnis, Introduction to Mineral Sciences, Cambridge University Press, New York, 1995, 457 pp.

[26] C. Medrano, M. Schlenker, J. Baruchel, J. Espeso, Y. Miyamoto, Domains in the low-temperature phase of magnetite from synchrotron-radiation x-ray topographs, Phys. Rev. B. 59 (1999) 1185–1195.

[27] J. Baruchel, E. Boller, J.I. Espeso, H. Klein, C. Medrano, J. Nogues, E. Pernot, M. Schlenker, Bragg-diffraction imaging of magnetic crystals with third-generation synchrotron radiation, J. Magn. Magn. Mater. 233 (2001) 38–47.

[28] B. Devouard, M. Pósfai, X. Hua, D.A. Bazylinski, R.B. Frankel, P.R. Buseck, Magnetite from magnetotactic bacteria: Size distributions and twinning, Am. Miner. 130 (1998) 1387–1398.

[29] P. Müllner, K. Ullakko, The force of a magnetic/electric field on a twinning dislocation, Phys. Stat. Sol. 208 (1998) R1–R2.

[30] P.J. Ferreira, J.B. Van der Sande, Magnetic field effects on twin dislocations, Scr. Mater. 41 (1999) 117–123.

[31] H. Träuble, The influence of crystal defects on magnetization processes in ferromagnetic single crystals, in: A.E. Berkowitz, E. Kneller (Eds.), Magnetism and Metallurgy, Academic Press, New York, 1969, pp. 622–687.

[32] L.R. Bickford Jr., Ferromagnetic resonance absorption in magnetite single crystals, Phys. Rev. 78 (1950) 449–457.

[33] H.J. Williams, R.M. Bozorth, M. Goertz, Mechanism of transition in magnetite at low temperatures, Phys. Rev. 91 (1953) 1107–1115.

[34] K. Moloni, B.M. Moskowitz, E.D. Dahlberg, Domain structures in single crystal magnetite below the Verwey transition as observed with a low-temperature magnetic force microscope, Geophys. Res. Lett. 23 (1996) 2851–2854.

[35] J.L. Tholence, R. Tournier, Susceptibility and remanent magnetization of a spin glass, J. Phys. 35 (C4) (1974) 229–235.

[36] A. Aharoni, E.P. Wohlfarth, The isothermal remanence (IRM) and the thermoremanence (TRM) of spin glasses, J. Appl. Phys. 55 (1984) 1664–1666.